

Cite this: *Soft Matter*, 2012, **8**, 827

www.rsc.org/softmatter

PAPER

Hydrogen-bonded multilayers of micelles of a dually responsive dicationic block copolymer

Irem Erel,^{†*} H. Enis Karahan,^a Cansel Tuncer,^b Vural Bütün^b and A. Levent Demirel^{*a}

Received 4th July 2011, Accepted 11th October 2011

DOI: 10.1039/c1sm06248d

We report the fabrication of hydrogen-bonded multilayers of micelles of a dually responsive, dicationic block copolymer, poly[2-(*N*-morpholino)ethyl methacrylate-*block*-2-(diisopropylamino)ethyl methacrylate] (PMEMA-*b*-PDPA). By taking advantage of the difference in the hydrophilicity of PMEMA and PDPA blocks, micelles with a PMEMA-corona and a PDPA-core were obtained above pH 6.5 and were assembled layer-by-layer at the surface with tannic acid (TA) at pH 7.4 through hydrogen bonding interactions between morpholino units of PMEMA and hydroxyl groups of TA. Destruction of PMEMA-*b*-PDPA micelles/TA films could be controlled at both acidic and basic conditions. At basic pH (pH = 8.75), multilayers disintegrated due to ionization of TA and disruption of hydrogen bonding interactions between layers of micelles and TA. At moderately acidic pH values, partially dissolved PMEMA-*b*-PDPA micelles and monomers underwent a restructuring with TA molecules and remained adsorbed at the surface. Complete dissolution of the multilayers occurred at around pH 3.6 due to further protonation of the tertiary amino groups on both blocks of PMEMA-*b*-PDPA, resulting in a charge imbalance between PMEMA-*b*-PDPA and TA layers followed by disintegration of the films. We have also encapsulated pyrene in the micellar cores and found that pyrene released from PMEMA-*b*-PDPA micelles/TA films increased 1.5- and 2.5-fold when the pH was decreased from 7.5 to 6 and 5, respectively. Such an increase in the amount of pyrene released was due to pH-controlled dissolution of the micellar cores. We have also found that at pH 7.5, increasing the temperature to 40 °C enhanced the release of pyrene by approximately 2-fold. Such an increase is due to lower critical solution temperature (LCST) behaviour of coronal PMEMA chains leading to temperature-induced conformational changes on the coronal chains, facilitating the release of pyrene through the coronal chains into the solution. Hydrogen bonded multilayers of micelles of a dicationic block copolymer are interesting due to the response of both multilayers and micellar cores at different pH paving the way for multiple pH-controlled delivery of functional molecules from surfaces.

Introduction

The layer-by-layer (LbL) technique-preparation of ultrathin films through alternating deposition of interacting materials-has become a versatile tool to prepare functional surfaces due to its simplicity, low cost and the possibility of preparing conformational coatings and incorporating functional molecules within the film structure.¹⁻⁴ Soon after its discovery, LbL polymer films became of interest to many researchers and found applications in areas from electronics⁵ to biomedical engineering.⁶ Rubner⁷ and Wang^{8,9} were first to introduce the use of hydrogen bonding

interactions as a driving force for multilayer build up, paving the way for the use of neutral polymers in LbL assembly. Taking advantage of hydrogen bonding interactions, Sukhishvili and Granick discovered so called “erasable films”-hydrogen-bonded multilayers of water-soluble neutral polymers and polyacids that can be completely released from the surface by increasing pH-and opened a new perspective in controlled release of functional molecules from surfaces.^{10,11}

One drawback of LbL films is that their loading capacity for poorly water soluble functional molecules is not high due to relatively hydrophilic nature of the water soluble polymer film components. Micellar aggregates with hydrophilic shell and hydrophobic core structures obtained through self-assembly of water-soluble amphiphilic block copolymers are ideal reservoirs to dissolve poorly water soluble drug molecules in their hydrophobic cores.¹² Therefore, block copolymer micelles (BCMs) are ideal building blocks to load poorly water soluble molecules into multilayer films at higher capacity compared to multilayers of

^aDepartment of Chemistry, Koç University, RumelifeneriYolu, 34450 Sariyer, Istanbul, Turkey. E-mail: erel@metu.edu.tr; Tel: +90 312 2103233; ldemirel@ku.edu.tr; +90 212 3381350

^bDepartment of Chemistry, Eskişehir Osmangazi University, 26480 Eskişehir, Turkey

[†] Present address: Middle East Technical University Department of Chemistry 06800 Çankaya, Ankara, Turkey

linear polymers. BCM containing electrostatically bound multilayers have been reported by many research groups.^{13–18} The first example of hydrogen-bonded multilayers containing BCMs was reported by Kim *et al.* in which they demonstrated inhibition of the growth of bacteria by diffusion controlled release of the antibacterial agent from the micellar cores when hydrogen-bonded multilayers of poly(ethylene oxide)-*block*-poly(ϵ -caprolactone) (PEO-*b*-PCL) micelles and polyacrylic acid (PAA) disintegrated under physiological conditions.¹⁹ In another study, Zhao and co-workers reported fabrication of hydrogen-bonded multilayers of PAA and micelles of PEO-*b*-poly[7-(2-methacryloyloxyethoxy)-4-methylcoumarin] (PCMA) and demonstrated tuning diffusion controlled release of Nile Red from the micellar cores by photocrosslinking of the PCMA-core blocks through dimerization of coumarin groups.²⁰

Unlike BCMs with cores composed of non-responsive polymers as discussed in the above studies,^{13–20} BCMs with stimuli responsive cores can release the preloaded cargo by simply changing the environmental conditions and dissolution of the micellar cores. In this context, Tan *et al.* demonstrated temperature-induced swelling transitions in electrostatic multilayers of PAA and micelles of poly(*N,N*-dimethylaminoethyl methacrylate)-*b*-poly(propylene oxide)-*b*-poly(*N,N*-dimethylaminoethyl methacrylate) (PDEA-*b*-PPO-*b*-PDEA) in which the transitions were induced by cycling the temperature below and above LCST of PPO.²¹ In another study, Zhu *et al.* LbL assembled PAA with poly(*N*-vinylpyrrolidone)-*b*-poly(*N*-isopropylacrylamide) (PVPON-*b*-PNIPAM) micelles with temperature-responsive PNIPAM cores through hydrogen bonding interactions and demonstrated similar swelling/deswelling transitions in the multilayers when the temperature was cycled above and below LCST of PNIPAM.²² BCMs with pH-responsive cores composed of polybasic blocks with tertiary amino groups attracted great attention due to their stability at neutral pH and dissolution near-below neutral pH values. The response of such BCM cores in moderately acidic environments is specifically important and promising due to the acidic nature of tumor tissues and local pH drops in the body induced by infection. Incorporation of BCMs with pH-responsive polybasic core blocks into electrostatically bound multilayer systems has earlier been shown in several studies.^{23–28} However, including such BCMs into hydrogen-bonded multilayers used to be a challenge due to different pH conditions required for hydrogen-bonded self-assembly (acidic conditions) and formation of micellar aggregates (above neutral pH). The first example of hydrogen-bonded multilayers of BCMs with polybasic cores was reported by Erel and Sukhishvili.²⁹ Taking advantage of their previous finding—the use of a natural polyphenol (TA) as the hydrogen donor and extension of film deposition pH range up to neutral values³⁰—they have recently demonstrated LbL films of micelles of poly(2-(diethylamino)ethyl methacrylate)-*block*-poly(*N*-isopropyl acrylamide) (PDEA-*b*-PNIPAM) with pH-responsive PDEA-cores and TA at a physiologically relevant pH of 7.5. In another study, Hammond and co-workers constructed hydrogen-bonded multilayers of TA and micelles of poly(ethylene oxide)-*b*-poly(2-hydroxyethyl methacrylate) (PEO-*b*-PHEMA) in which the PHEMA-core block was conjugated to doxorubicin (PEO-*b*-PHEMA-dox). Different from the work of Erel *et al.*, in this study, not the micelle core blocks but the carbamate linkage between

doxorubicin and PHEMA-core chains exhibited pH-response resulting in the release of doxorubicin at acidic pH while PEO-*b*-PHEMA micelles remained completely intact within the multilayers.³¹

All above-mentioned studies of hydrogen-bonded multilayers containing polymeric micelles obtained from diblock copolymers having at least one hydrophilic, hydrogen accepting neutral block with no polyelectrolytic property forming the micellar coronas. In this study, unlike micelles of a diblock copolymer with at least one hydrophilic and neutral block, we report on incorporation of micelles of a diblock copolymer made up of two cationic blocks into hydrogen-bonded multilayers. Taking advantage of the difference in the hydrophilicity and pK_a values between the two polybasic blocks of the copolymer, we were able to obtain BCMs with polybasic cores and hydrophilic hydrogen accepting coronas at/above slightly acidic conditions ($pH \geq 6.5$). Using a polyphenol as the hydrogen donor, we were able to construct hydrogen-bonded multilayers of such BCMs at a pH range of 6.5–7.5. Introduction of micelles of block copolymers with solely polybasic blocks allowed control of the destruction of hydrogen-bonded films at both acidic and basic conditions. Moreover, we show that the amount of functional molecules released from the micellar cores can be controlled by temperature through temperature-induced conformational changes on the coronal blocks.

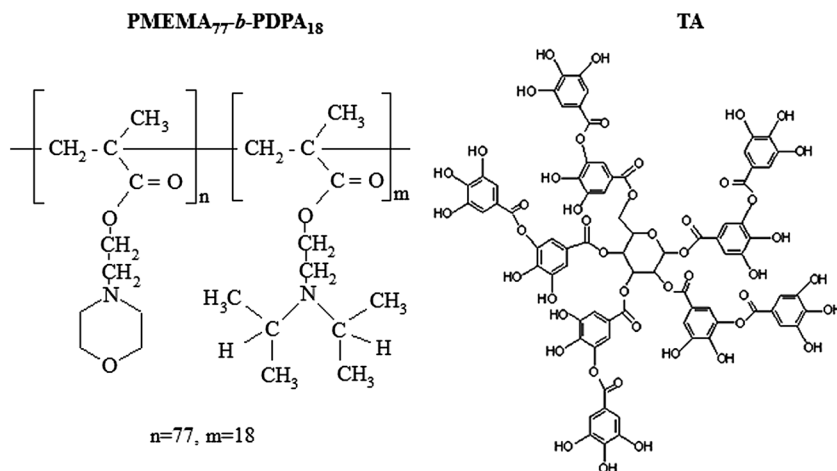
As far as we are aware, this is the first study showing the incorporation of micelles of a block copolymer with solely polybasic blocks into hydrogen-bonded multilayers providing control of dissolution of the films at opposite pH ranges and the effect of temperature-induced conformational changes of coronal chains on the release of a hydrophobic functional molecule from the micellar cores. This study contributes to the understanding of the effect of physical parameters on stimuli-response characteristics of hydrogen-bonded multilayers and scrutinizes the chemical structure–property relationship of hydrogen-bonded films. Considering the response of BCM cores and multilayers at different pH values, this work may serve as a model system for multiple pH-controlled delivery of functional molecules from surfaces.

Experimental

Materials

Branched polyethylene imine (BPEI, M_w : 25,000 Da) and pyrene were purchased from Sigma-Aldrich Chemical Co. Tannic acid (TA; M_w : 1701.20 Da), hydrochloric acid, sodium hydroxide and monobasic sodium phosphate were purchased from Merck Chemicals. All chemicals were used as received. The deionized (DI) water was purified by passage through a Milli-Q system (Millipore).

Synthesis and characterization of PMEMA₇₇-*b*-PDPA₁₈. The PMEMA-*b*-PDPA diblock copolymer was synthesized using group transfer polymerization (GTP) as described elsewhere.^{32,33} The chemical structure of the PMEMA-*b*-PDPA diblock is given in Scheme 1. The molecular weight and the polydispersity index of this copolymer were determined to be 19 400 g mol⁻¹ and 1.10, respectively, as measured by gel permeation chromatography



Scheme 1 Chemical structures of PMEMA₇₇-*b*-PDPA₁₈ and TA.

(GPC) with THF eluent at a flow rate of 1.0 mL min⁻¹ using PMMA calibration standards. The PDPA content was 20 mol %, as judged by proton NMR spectroscopy. On the basis of end group analysis, the mean degrees of polymerization were calculated to be 77 for the PMEMA block and 18 for the PDPA block, respectively.

Preparation of PMEMA₇₇-*b*-PDPA₁₈ micelles. 0.5 mg mL⁻¹ PMEMA₇₇-*b*-PDPA₁₈ solution was prepared by dissolving PMEMA₇₇-*b*-PDPA₁₈ in 0.01 M NaH₂PO₄ buffer at pH 2. PMEMA₇₇-*b*-PDPA₁₈ micelles were obtained above pH 6.5, at 25 °C by gradually increasing the solution pH with 0.1 M NaOH.

Dynamic light scattering (DLS) and ξ -potential measurements of PMEMA₇₇-*b*-PDPA₁₈ micelles in aqueous solution. Hydrodynamic size measurements of PMEMA₇₇-*b*-PDPA₁₈ solution were performed in aqueous solution using Zetasizer Nano-S (Malvern Instruments Ltd.). Number average hydrodynamic diameters of the micelles were generated *via* cumulants analysis of the auto-correlation data. The zeta potential value of PMEMA₇₇-*b*-PDPA₁₈ micelles at pH 7.5 was obtained from electrophoretic mobility values through the Smoluchowski approximation using the Brookhaven ZetaPALS Instrument. For both DLS and ξ -potential measurements, PMEMA₇₇-*b*-PDPA₁₈ was dissolved in 0.01 M NaH₂PO₄ solution with a final concentration of 0.5 mg mL⁻¹.

Deposition of multilayers for ellipsometry, atomic force microscopy (AFM), scanning electron microscopy (SEM) and fluorescence spectroscopy. Silicon wafers were kept in a UV-ozone cleaner (Model 42-220 Jelight Company, Inc.) for 2 h and rinsed with DI water. After treating with concentrated sulfuric acid and rinsing with DI water, wafers were immersed in 0.25 M NaOH solution followed by rinsing with DI water and drying under a flow of nitrogen. 0.5 mg mL⁻¹ BPEI, PMEMA₇₇-*b*-PDPA₁₈ and TA solutions were prepared in 0.01 M NaH₂PO₄ solution at pH 2. One bilayer of BPEI and TA, both deposited at pH 5.5, was used as a precursor layer prior to film deposition. PMEMA₇₇-*b*-PDPA₁₈ micelles/TA multilayers were deposited at pH 7.4 by alternatingly immersing the silicon wafer or glass

substrates into polymer solutions for 15 min followed by 2 intermediate rinsing steps. The pH stability of the films was followed by exposing the films to 0.01M NaH₂PO₄ or 0.01 M Na₂HPO₄ solutions of either decreasing or increasing pH. The thickness of the dry films was measured by a Microphotronics ELX-01R ellipsometer using 632.8 nm laser light at a 70° angle. AFM imaging of PMEMA₇₇-*b*-PDPA₁₈ micelles/TA films was performed by NT-MDT Solver P47 AFM in tapping mode using Si cantilevers. Release of pyrene from 20-bilayers double sided PMEMA₇₇-*b*-PDPA₁₈ micelles/TA films was monitored using fluorescence spectrometry (Horiba JobinYvon FluoroMax-3). Aliquots (~3 mL) were taken from the solutions which the multilayer coated substrates were immersed into at certain time intervals. Pyrene was excited at 335 nm and the fluorescence emission intensity at $\lambda = 375$ nm was used to monitor the pyrene released from the multilayers into the solution as a function of time. Cross-sectional SEM imaging of 10-bilayers PMEMA₇₇-*b*-PDPA₁₈ micelles/TA films was performed by using Zeiss LEO Supra VP35 FE-SEM after carbon coating.

Results and discussion

1. Aqueous solution properties of PMEMA₇₇-*b*-PDPA₁₈

To optimize the film preparation conditions for PMEMA₇₇-*b*-PDPA₁₈/TA films and understand the characteristics of multilayers, we studied aqueous solution properties of PMEMA₇₇-*b*-PDPA₁₈ prior to film fabrication. Note that a detailed investigation of solution properties of PMEMA₇₇-*b*-PDPA₁₈ has earlier been demonstrated by Bütün *et al.*^{32,33}

PMEMA₇₇-*b*-PDPA₁₈ is composed of two weak polybasic blocks (see Scheme 1). In addition to the pH-response of both blocks which arises from the tertiary amino groups of both PMEMA and PDPA blocks, PMEMA is temperature-responsive and exhibits a lower critical solution temperature within a range of 34–54 °C at pH 7 depending on its molecular weight.^{32,33} Therefore, PMEMA₇₇-*b*-PDPA₁₈ is soluble in water at room temperature and acidic pH when both blocks are in the protonated form. Unlike PDPA which precipitates in water above its pK_a of 6.4 due to deprotonation of the tertiary amino

groups, PMEMA ($pK_a \sim 4.9$) is soluble in water up to pH 12.³³ The difference in the hydrophilicity of the blocks of this dicationic block copolymer enables PMEMA₇₇-*b*-PDPA₁₈ to self-assemble into micellar aggregates above pH 6.5 with the water insoluble PDPA block forming the core and the hydrophilic PMEMA block forming the corona.³³ Fig. 1 shows pH-triggered micellization and demicellization of PMEMA₇₇-*b*-PDPA₁₈ at 25 °C. Micellization of PMEMA₇₇-*b*-PDPA₁₈ was reversible but showed some hysteresis just below the critical micellization pH. The hydrodynamic size of PMEMA₇₇-*b*-PDPA₁₈ was higher in a pH range of 6.5–5.5 when the pH was decreased compared to that when pH was increased. The reason for the gradual depletion of the aggregation number within this pH range during demicellization can be attributed to inter- and intra- molecular hydrophobic association between the unprotonated PDPA core blocks suppressing the reprotonation of the tertiary amino groups of PDPA resulting in partial removal of PMEMA₇₇-*b*-PDPA₁₈ monomers from the micellar aggregates just-below the critical pH. Thus, it was necessary to further lower the pH to reach the critical ionization degree for complete molecular dissolution of the PMEMA₇₇-*b*-PDPA₁₈ micelles. Note that during micellization/demicellization, just below/just above critical pH, unimers and micelles exist together in the solution.

We have also explored the effect of temperature on the colloidal stability of the micellar dispersion of PMEMA₇₇-*b*-PDPA₁₈ at neutral and moderately acidic pH values. Fig. 2 shows the change in the hydrodynamic size of PMEMA₇₇-*b*-PDPA₁₈ with increasing temperature at certain pH values. At pH 7.5, we observed a cloud point at 31 °C for PMEMA₇₇-*b*-PDPA₁₈ micelles due to loss in water solubility of the coronal PMEMA blocks which were responsible for dispersion stability in an aqueous medium. It was previously reported that LCST of the PMEMA homopolymer was 34–54 °C at pH 7 depending on its molecular weight.³³ We have also monitored the evolution of the hydrodynamic size of PMEMA homopolymer with a molecular weight similar to that of PMEMA coronal blocks of PMEMA₇₇-*b*-PDPA₁₈ micelles and recorded its cloud point as ~48 °C in aqueous solution at pH 7.5. The observation of a lower cloud point temperature for PMEMA₇₇-*b*-PDPA₁₈ micelles was because of an increase in the hydrophobic content of the polymer chains arising from already unprotonated PDPA blocks. We then prepared PMEMA₇₇-*b*-PDPA₁₈ micelles at pH 6.75 which

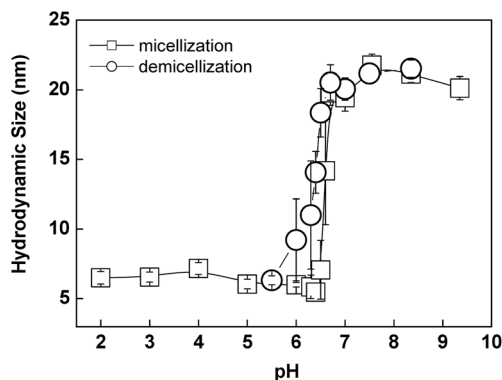


Fig. 1 pH-Triggered micellization/demicellization of 0.5 mg mL⁻¹ PMEMA₇₇-*b*-PDPA₁₈ at 25 °C.

was only 0.25 pH units higher than the critical micellization pH at 25 °C. At this pH, tertiary amino groups on PDPA are partially protonated and increase the hydrophilic content of the block copolymer resulting in a shift of the cloud point up to 35 °C. Note that PMEMA and PDPA have pK_a 's of 4.9 and 6.4, respectively.^{32,33} The change in charge density on PDPA chains is higher than that on PMEMA chains when the pH was decreased from 7.5 to 6.75 and 6.0. Therefore, we correlate this increase in the cloud point with decreasing pH mostly to changes in the charge density on PDPA blocks rather than PMEMA blocks. At pH 6, when both blocks molecularly dissolved in aqueous solution, the cloud point shifted even up to ~48 °C. However, when the pH was further decreased to 5, we did not observe a cloud point between 25–65 °C. Interestingly, we detected aggregates of ~17 nm between 31–48 °C at pH 6.

Considering the fact that PMEMA exhibits LCST behaviour, those micelles possibly have PMEMA-core and cationic PDPA-corona structures. At this pH, as proton NMR studies indicated (not shown), PMEMA block is in a neutral form and has a thermo-responsive nature but the PDPA block is mainly protonated and has good solubility. Thus, an increase in temperature resulted in the dehydration of the PMEMA block and PMEMA-core micelle formation before aggregation at 48 °C. Similarly to PMEMA-*b*-PDEA diblock copolymer as reported before,³⁴ PMEMA-*b*-PDPA diblock copolymer can form both pH-induced PDPA-core micelles and temperature-induced PMEMA-core reverse micelles in aqueous media. This observation allows us to define the PMEMA-*b*-PDPA diblock copolymer as a novel “schizophrenic” diblock copolymer as well.

2. Preparation of PMEMA₇₇-*b*-PDPA₁₈ micelles/TA films

We then focused on fabrication of LbL films of PMEMA₇₇-*b*-PDPA₁₈ micelles and TA through hydrogen bonding interactions. TA is a water soluble polyphenol with a pK_a of ~8.5³⁰ and has 25 phenolic hydroxyl groups per molecule capable of acting as hydrogen donors. Based on an approach of a decrease in the charge density of the ionizable hydrogen donating polyacid at neutral pH values, Erel and Sukhishvili reported earlier the possibility of the construction of hydrogen-bonded multilayers within a pH range of 2–7.5 using TA instead of mostly used polycarboxylic acids with lower pK_a values. PMEMA blocks of PMEMA₇₇-*b*-PDPA₁₈ micelles have morpholino units on the side chains and accommodate both ether oxygens and tertiary amino groups. Although amines are stronger hydrogen acceptors than ethers,³⁵ both of them can act as hydrogen acceptors in principle, thus PMEMA coronal chains of PMEMA₇₇-*b*-PDPA₁₈ micelles may form hydrogen bonds through both ether oxygens and the unprotonated tertiary amino groups. To ensure deposition of PMEMA₇₇-*b*-PDPA₁₈ in the micellar morphology, we prepared LbL films of PMEMA₇₇-*b*-PDPA₁₈ micelles and TA at pH 7.5, above the critical micellization pH of 6.5. At a pH of 7.5, well above the pK_a of PMEMA (pK_a of PMEMA ~ 4.9), tertiary amino groups of PMEMA coronal blocks are in the unprotonated state. PMEMA₇₇-*b*-PDPA₁₈ micelles gave a slightly negative ξ -potential value of ~ -4.88 mV, probably due to the binding of anions of the buffer salt (NaH₂PO₄) onto coronal chains and/or the core surface. The fact that PMEMA₇₇-*b*-PDPA₁₈ micelles did not show a positive zeta potential at pH

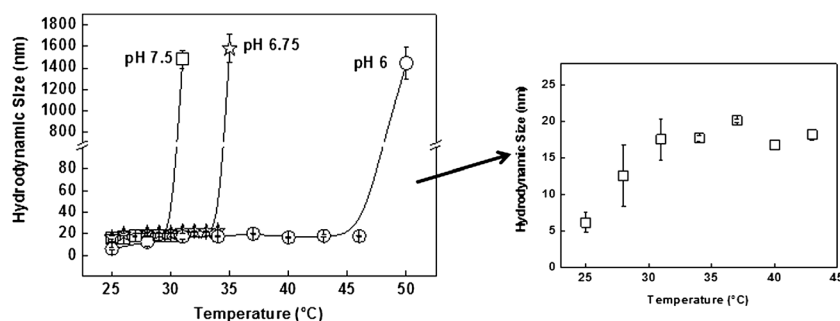


Fig. 2 Evolution of hydrodynamic size of PMEMA_{77-b}-PDPA₁₈ with increasing temperature at pH 7.5, pH 6.75 and pH 6.0.

7.5 suggests that contribution of electrostatic interactions between protonated tertiary amino groups of PMEMA and phenolate ions of TA to the film growth is out of the question. Therefore, the driving force for the construction of PMEMA_{77-b}-PDPA₁₈ micelles/TA multilayers should be mainly hydrogen bonding interactions between morpholino units of PMEMA and hydroxyl groups of TA.

Fig. 3-Panel A shows the evolution of the thickness of multilayers of PMEMA_{77-b}-PDPA₁₈ micelles and TA with increasing number of layer pairs. Multilayers of PMEMA_{77-b}-PDPA₁₈ micelles and TA showed exponential growth.

Fig. 3-Panel B shows the 2 $\mu\text{m} \times 2 \mu\text{m}$ area AFM height images of PMEMA_{77-b}-PDPA₁₈ micelles/TA films. The height histograms of these images are seen in Fig. 3-Panel B (d) as an inset which shows slightly increased surface roughness for 6 and 9 bilayer compared to 3 bilayer films. The increase in roughness with increasing number of bilayers was more significant at larger length scales. Fig. 3-Panel B (d) shows the height histograms of 10 $\mu\text{m} \times 10 \mu\text{m}$ area AFM scans for 3, 6, 9, and 12 bilayer films. The surface roughness increased as the number of bilayers went from 3 to 12. This can be understood by the irregular packing of micelles starting from the first layer combined with the adsorption kinetics. When an irregularly packed incomplete micelle layer with holes is allowed to interact with TA molecules and then again with the micellar solution, the probability of adsorbing on higher parts of the surface at first encounter will be larger than going into the holes. Weakly associating morpholino units and protonated TA molecules are also expected to contribute to the rough and loose film structure. As more layers are added, then the surface roughness will be amplified. An increased surface area may also lead to exponential growth which was also observed in our case.

An exponential growth regime has earlier been observed by others^{21,36-41} and was correlated with either surface roughness⁴⁰ or diffusion of at least one of the film components in and out during multilayer deposition^{36,41} resulting in higher amounts of material deposited at the surface with increasing number of layers. Considering the fact that PMEMA_{77-b}-PDPA₁₈ micelles were not single polymer chains but formed through aggregation of many polymer chains, we suggest that diffusion of PMEMA_{77-b}-PDPA₁₈ micelles in and out throughout the film structure is unlikely. Thus, we attribute the exponential growth observed for PMEMA_{77-b}-PDPA₁₈ micelles/TA films to high surface roughness resulting from irregular micelle packing together with weakly associating morpholino units and protonated TA

molecules leading to a rough and loose film structure. For electrostatically bound multilayers, Shiratori and Rubner reported that lower number of ionic cross-links between the layers within a film structure led to a higher number of loops resulting in increased surface roughness, thus surface roughness could be indirectly correlated with the conformational state of the multilayers.⁴² For hydrogen-bonded systems, Sukhishvili reported on the correlation between the lower number of binding points between the layers and loopy conformation of polymer layers for weakly associating hydrogen donating/accepting polymer pairs.⁴³

In contrast to PMEMA_{77-b}-PDPA₁₈ micelles/TA system, a study by Erel *et al.* demonstrated a linear growth profile for multilayers of PNIPAM-*b*-PDEA micelles and TA self-assembled through hydrogen bonding interactions between the PNIPAM-corona and TA.²⁹ This contrast in the growth profile of PMEMA_{77-b}-PDPA₁₈ micelles/TA and PNIPAM-*b*-PDEA micelles/TA films can be explained by the difference in the binding strength of hydrogen accepting polymers in these two systems. Carbonyl groups of PNIPAM are stronger hydrogen acceptors and associates with TA molecules stronger than morpholino units of PMEMA resulting in a higher number of binding points between the layers and thinner films. Kharlamieva and Sukhishvili also reported earlier that weakly associating polymer pairs [*e.g.* PEO/polycarboxylic acid] form thicker films than strongly associating polymer pairs [*e.g.* poly(vinyl caprolactam) (PVCL)/polycarboxylic acid].⁴³

3. pH-Triggered dissolution of PMEMA_{77-b}-PDPA₁₈ micelles/TA multilayers

pH-Stability of PMEMA_{77-b}-PDPA₁₈ micelles/TA films was followed in two different regions: i) the basic pH region: a 6-bilayer PMEMA_{77-b}-PDPA₁₈ micelles/TA film which was deposited at pH 7.4 was exposed to increasing pH values; ii) the acidic pH region: a 6-bilayer PMEMA_{77-b}-PDPA₁₈ micelles/TA film which was deposited at pH 7.4 was exposed to decreasing pH values. Fig. 4 shows pH-triggered dissolution of PMEMA_{77-b}-PDPA₁₈ micelles/TA both at basic and acidic regions.

At the basic region, critical dissolution pH (the pH at which $\geq 10\%$ loss in film thickness occurs) for PMEMA_{77-b}-PDPA₁₈ micelles/TA films was recorded as ~ 8.75 . Dissolution of multilayers at a basic pH was due to ionization of TA ($pK_a \sim 8.5$) and loss of hydrogen bonding interactions between PMEMA coronal chains and TA resulting in the release of PMEMA_{77-b}-PDPA₁₈

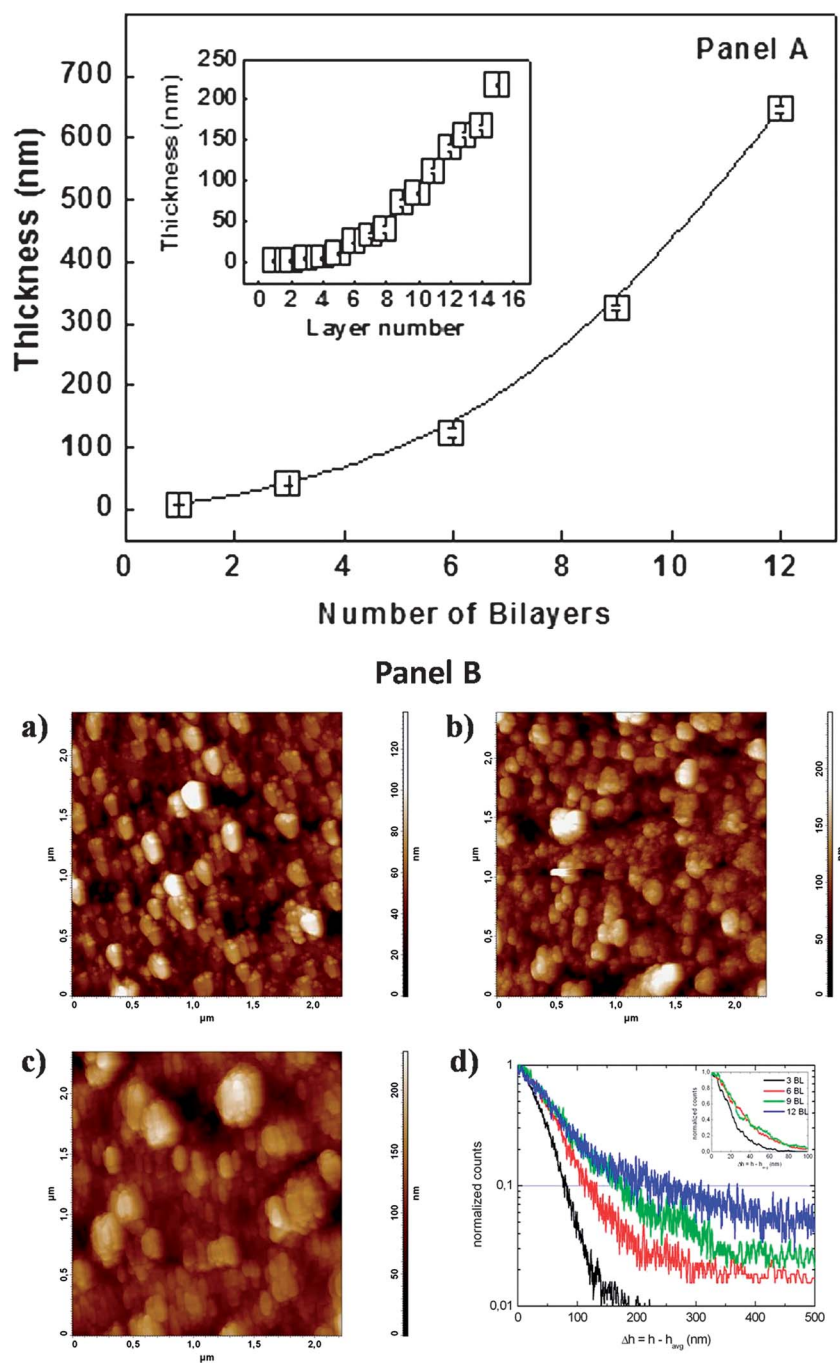


Fig. 3 **Panel A:** Film thickness vs. number of bilayers as obtained by ellipsometry. Inset shows layer-by-layer growth of PMEMA₇₇-*b*-PDPA₁₈ micelles/TA multilayers up to 8 bilayers. **Panel B:** 2 $\mu\text{m} \times 2 \mu\text{m}$ area AFM height images of PMEMA₇₇-*b*-PDPA₁₈ micelles/TA films: (a) 3 bilayers, (b) 6 bilayers, (c) 9 bilayers, (d) height histograms of 10 $\mu\text{m} \times 10 \mu\text{m}$ area AFM scans showing increased surface roughness as the number of bilayers goes from 3 to 12. The inset shows the height histograms of the AFM images in (a)-(c).

micelles and TA into the solution. The critical pH of 8.75 is in good agreement with the critical dissolution pH of 8.5 reported for the PEO/TA system in which multilayers were bound also through hydrogen bonding between ether oxygens and phenolic hydroxyl groups.³⁰ We suggest that this slight difference in the critical pH values of PMEMA₇₇-*b*-PDPA₁₈ micelles/TA and PEO/TA films may be due to the difference in the binding strength between the layers. In PMEMA₇₇-*b*-PDPA₁₈ micelles/

TA films, PMEMA coronal chains can participate in hydrogen bonding through both unprotonated tertiary amino groups and ether oxygens, while in PEO/TA films, PEO only binds from ether oxygens and this difference between the hydrogen accepting capability of hydrogen acceptors might have resulted in a higher number of binding points between the layers in PMEMA₇₇-*b*-PDPA₁₈ micelles/TA films and enhanced stability in the pH-scale. In addition, the cyclic nature of the morpholine

molecules of PMEMA blocks whose ether oxygens might be more accessible for hydrogen bonding resulting in higher number of binding points between the layers may also account for the observed difference. It has been reported that oxygen atoms of cyclic ethers are more exposed to water for hydrogen bonding, therefore are more soluble in water compared to aliphatic ethers.⁴⁴ Searles and Tamres also demonstrated that cyclic ethers, except the ethylene oxides, can act as hydrogen acceptors as good or better than comparable unbranched acyclic ethers and their hydrogen accepting strength depends strongly on the ring size.⁴⁵

At acidic regions, critical dissolution pH for PMEMA₇₇-*b*-PDPA₁₈ micelles/TA films was recorded as pH 3.6. Different from film destruction at basic pH values due to ionization of TA molecules, dissolution of multilayers at acidic pH was due to protonation of both PDPA and PMEMA blocks. To understand the dissolution mechanism, destruction of multilayers in the acidic region can be examined in 2 different subregions: the region between pH 7.5–4 and the region between pH 4–2.

In the region between pH 7.5 to pH 4, we did not record any loss in the material deposited at the surface. A slight increase in film thickness was recorded between pH 5.2–4. Protonation of PMEMA and PDPA blocks with decreasing pH might have resulted in an increase in the hydrophilicity of the multilayer matrix and entrapment of water molecules which probably caused a slight increase in film thickness. As discussed in Section 1 (Fig. 1), complete demicellization in aqueous solution occurred at pH 5.5. Therefore between pH 7.4–6.5 mainly micelles, at pH 6.5–5.5 both smaller micelles and unimers, and at pH 5.5–4 unimers should be present within the film. The reason for the conservation of the film thickness between pH 6.5–5.5 should be due to restructuring between TA and PMEMA₇₇-*b*-

PDPA₁₈ monomers which partially dissociated from the micellar aggregates as well as the remaining smaller micelles within the multilayers rather than removal of the monomers into the solution. Similarly, between pH 5.5–4, a restructuring between unimers and TA molecules can be pronounced. Note that enhanced ionization of polyacids in the presence of polycations has been reported.⁴⁶ Based on this fact, it was highly possible that hydroxyl groups of TA existed both in ionized and nonionized form at this pH range in the presence of partially protonated PDPA blocks. Therefore, in addition to hydrogen bonding, electrostatic interactions between amino groups of PMEMA and ionized hydroxyl groups of TA can also be pronounced. Another scenario for the conservation of the film thickness can be built on the preservation of the micellar morphology within the multilayers due to further protonation of TA and enhanced hydrogen bonding interactions between the PMEMA-coronal blocks and TA at decreasing pH resulting in restricted conformational changes in the micellar core blocks as previously observed by Erel *et al.*²⁹ Therefore, to further examine pH-induced changes within the multilayer structure, we have employed a cross-sectional SEM imaging technique to 10-bilayer PMEMA₇₇-*b*-PDPA₁₈ micelles/TA films. Fig. 5 shows cross sectional SEM images of multilayers at pH 7.5 and pH 5. The size of white domains observed at pH 7.5 were in good agreement with the hydrodynamic size of the micelles obtained from DLS measurements, therefore we attributed them to PMEMA₇₇-*b*-PDPA₁₈ micelles incorporated within the multilayers (Fig. 5A and 5B). Those white domains disappeared at pH 5, supporting the scenario based on dissolution of the micelles and a restructuring between PMEMA₇₇-*b*-PDPA₁₈ unimers/partially dissolved PMEMA₇₇-*b*-PDPA₁₈ micelles and TA (Fig. 5C).

Note that our results obtained from pH-triggered release of pyrene from PMEMA₇₇-*b*-PDPA₁₈/TA multilayers which will be discussed in detail in Section 4 also support dissolution of the micellar cores and a rearrangement within the multilayers between pH 5.5–4.

Finally, in the more acidic region (between pH 4–2), we observed a sharp decrease in the film thickness between pH 4 and pH 3.6 followed by a gradual erosion of the film between pH 3.6 and pH 2. Decreasing pH below 4 significantly increased the charge density on both PDPA ($pK_a = 6.4$) and PMEMA ($pK_a = 4.9$) blocks resulting in a charge imbalance between PMEMA₇₇-*b*-PDPA₁₈ and TA layers in the film structure. Electrostatic repulsion between charged PMEMA₇₇-*b*-PDPA₁₈ chains as well as increased osmotic pressure within the multilayers due to penetration of the counterions to compensate the created excess positive charge resulted in destruction of the film. Dissolution of multilayers caused by charge imbalance has been reported by others, too.^{47–49}

In contrast to our findings, Erel and Sukhishvili reported that in multilayers of micelles of PNIPAM₂₀₀-*b*-PDEA₇₀ and TA, binding of TA largely inhibited dissolution of PNIPAM₂₀₀-*b*-PDEA₇₀ micelles at low pH due to further protonation of TA hydroxyl groups. In their study, the enhanced hydrogen bonding interactions between carbonyl groups of PNIPAM-corona and hydroxyl groups of TA at low pH restricted the pH-induced conformational changes in the micellar core blocks. Also, different from our system, no mass loss was recorded in that study even at highly acidic conditions.²⁹ The difference in the

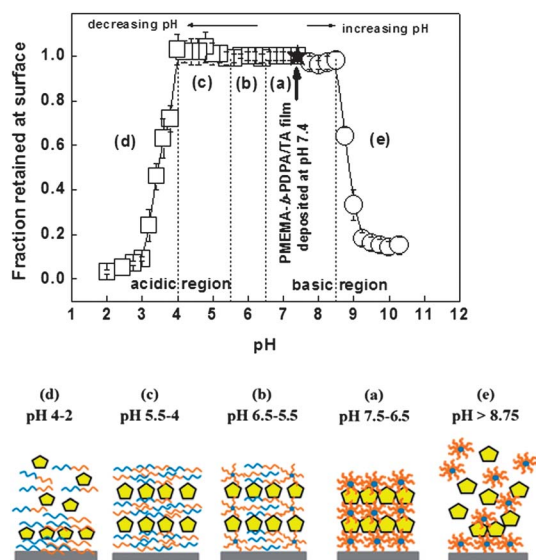


Fig. 4 pH-Triggered dissolution of PMEMA₇₇-*b*-PDPA₁₈ micelles/TA films (deposition pH \sim 7.4) at basic or acidic regions. The fraction retained at the surface was calculated from the equilibrated values of film thickness at each pH value. Error bars are within symbol if not shown. Fraction at pH 7.4 is shown with a filled star and is the starting point of the dissolution curves for both basic and acidic regions. Images represent dissolution of PMEMA₇₇-*b*-PDPA₁₈ micelles/TA multilayers at different pH intervals.

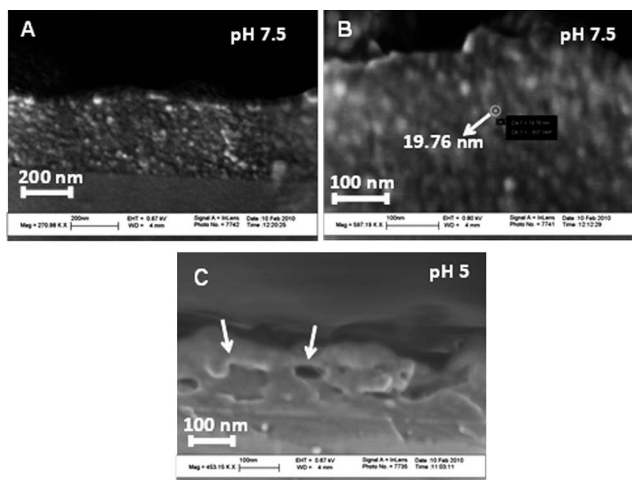


Fig. 5 Cross-sectional SEM images of PMEMA₇₇-*b*-PDPA₁₈ micelles/TA films after exposure to pH 7.5 (A and B) and pH 5 (C).

dissolution characteristics of PNIPAM₂₀₀-*b*-PDEA₇₀ micelles/TA and PMEMA₇₇-*b*-PDPA₁₈ micelles/TA might have resulted from: i) the difference in strength of hydrogen bonding between the layers determined by the chemical nature of hydrogen accepting polymers—carbonyl groups of PNIPAM are stronger hydrogen acceptors than amines and ether groups of PMEMA; ii) the difference in the charge density of PNIPAM₂₀₀-*b*-PDEA₇₀ and PMEMA₇₇-*b*-PDPA₁₈ at acidic pH values. PMEMA₇₇-*b*-PDPA₁₈, which is composed of two cationic blocks, bears higher positive charge density at an acidic pH than PNIPAM₂₀₀-*b*-PDEA₇₀ having only one cationic block and exceeded the critical charge density threshold for dissolution of the multilayers. Also, the higher charge density caused a higher osmotic pressure of the counterions and swelling of the PMEMA₇₇-*b*-PDPA₁₈/TA system resulting in complete dissolution of the multilayers above the critical charge density.

4. Effect of pH and temperature on release of pyrene from PMEMA₇₇-*b*-PDPA₁₈ micelles/TA multilayers

We encapsulated pyrene in PMEMA₇₇-*b*-PDPA₁₈ micelles prior to multilayer construction and monitored the pH-triggered release of pyrene from PMEMA₇₇-*b*-PDPA₁₈ micelles/TA multilayers both at 25 °C and 40 °C (Fig. 6). Pyrene was primarily included in the hydrophobic cores of PMEMA₇₇-*b*-PDPA₁₈ micelles, however it is possible that some amount could have also adsorbed on the PMEMA-coronal chains due to hydrophobic–hydrophobic interactions between pyrene and the hydrophobic polymer backbone. Note that all PMEMA₇₇-*b*-PDPA₁₈/TA films were prepared in the same batch to minimize the variation in the amount of pyrene loaded within the films between the samples. For fluorescence intensity measurements, samples were taken from the solution at specific time intervals in which the 20-bilayer PMEMA₇₇-*b*-PDPA₁₈/TA multilayers were immersed in. Fig. 6A shows the evolution of fluorescence intensity at pH 7.5, 6 and 5 at 25 °C. Release of pyrene at pH 7.5, when PMEMA₇₇-*b*-PDPA₁₈ was in the micellar form and multilayers were completely stable, (film deposited at pH = 7.4)

was low and based on self-diffusion of the pyrene molecules from the micellar cores. At pH 6, fluorescence intensity of the pyrene released into the solution was almost 1.5 times higher than the release at pH 7.5. We attribute this increase to partial dissolution of the micellar cores and removal of PMEMA₇₇-*b*-PDPA₁₈ monomers due to protonation of the PDPA blocks resulting in a restructuring within the multilayers and simultaneous release of the pyrene into the solution. At pH 5, intensity of pyrene released from the multilayers was around 2.3 and 1.5 times higher than the release at pH 7.5 and pH 6, respectively, associated with complete dissolution of the micellar cores triggering the release of pyrene into the solution. At all pH values, pyrene release profiles gradually levelled off. Pyrene release was completed in ~4 h at pH 5, slightly faster than those at pH 6 and pH 7.5 which took ~6 h.

We have also monitored the release of pyrene from 20 bilayers of PMEMA₇₇-*b*-PDPA₁₈ micelles/TA multilayers at 40 °C (Fig. 6B). At pH 7.5 and 40 °C, we found an increase in the amount of pyrene released from the multilayers. As seen in Fig. 2, critical temperature for PMEMA coronal blocks at pH 7.5 is ~31 °C. We suggest 2 possibilities for the increase in the amount of pyrene released at pH 7.5 and 40 °C: i) at 40 °C and pH 7.5, PMEMA coronal blocks might have phase separated and this conformational rearrangement within the multilayers might have facilitated the self-diffusion of pyrene from the micellar cores through PMEMA chains into the solution; ii) although

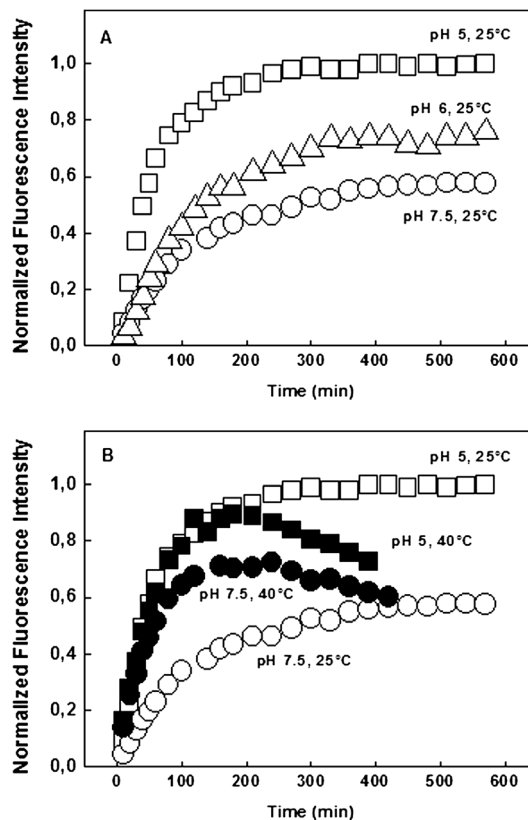
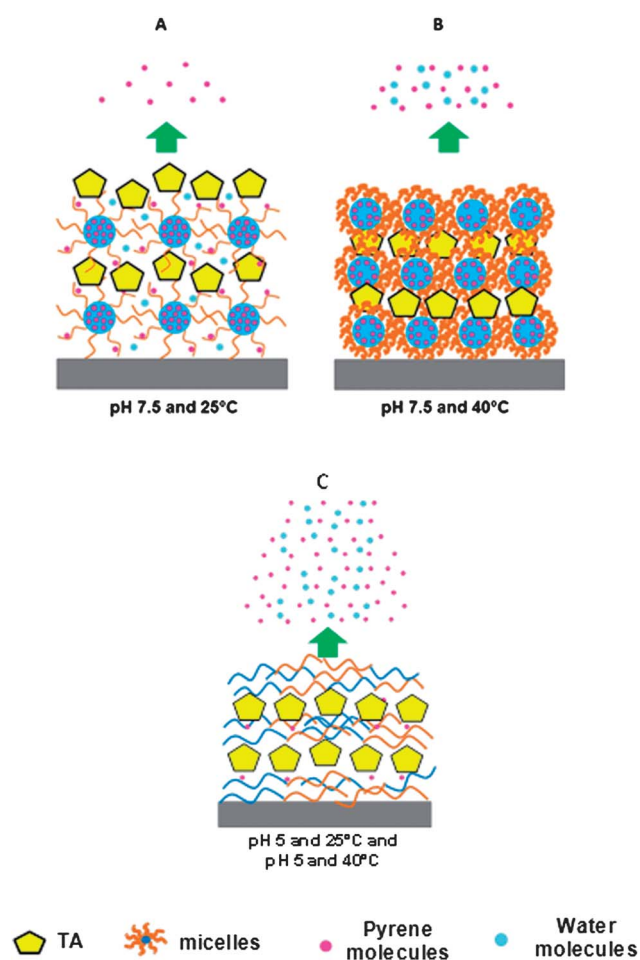


Fig. 6 Panel A: pH-triggered release of pyrene from PMEMA₇₇-*b*-PDPA₁₈ micelles/TA multilayers at pH 7.5, 6 and 5 at 25 °C Panel B: pH-triggered release of pyrene from PMEMA₇₇-*b*-PDPA₁₈ micelles/TA multilayers at pH 7.5 and 5 at 40 °C.

poorly soluble in water, pyrene molecules adsorbed on PMEMA coronal chains through hydrophobic interactions could have been removed by the water molecules into the solution due to loss of PMEMA–water interactions above the critical temperature (Scheme 2). Note that Sukhishvili and co-workers also reported that permeability of hydrogen-bonded PVCL/PMAA and PVME/PMAA multilayers for thymolblue increased with rising temperature and correlated this fact with deswelling of PVME and PVCL chains at temperatures near and above the LCST and formation of voids within the multilayers resulting in an increase in dye permeability. At pH 5 and 40 °C where PMEMA does not exhibit LCST behaviour, we did not observe significant differences in the amount of pyrene released. As seen in Fig. 6B, fluorescence intensity decreased gradually after ~3 h due to enhanced quenching of the fluorescence at high temperatures. In the first 2 h, fluorescence intensity was dominated by the continuous release of the encapsulated dye into the solution and the quenching effect could not be detected. As can be clearly seen for the data taken at pH 5, the fluorescence intensity was nearly the same (independent of temperature) for the first 2 h beyond which it was slightly less for $T = 40$ °C compared to $T = 25$ °C. After 3 h, as the release of pyrene levelled off, quenching was dominant and the fluorescence intensity decreased in time.



Scheme 2 Schematic representation of the release of pyrene from PMEMA₇₇-*b*-PDPA₁₈ micelles/TA films at pH 7.5, 25 °C (**A**); pH 7.5, 40 °C (**B**); pH 5, 25 °C and pH 5, 40 °C (**C**).

Conclusions

We have shown that by using micelles of a dicationic block copolymer as building blocks in hydrogen-bonded LbL self-assembly, we were able to introduce different critical pH values into the same system. At basic pH, intact micelles could be released from the multilayers due to ionization of the polyacid and loss in hydrogen bonding interactions between the layers. At acidic pH, we found that micellar cores could be simply dissolved below the critical micellization pH, while the multilayers remained attached at the surface. Further decreasing the pH below 4 resulted in complete disintegration of the multilayers due to protonation of the tertiary amino groups on both blocks of the copolymer imparting a charge imbalance within the film. We have also shown that the amount of functional molecules released from the micellar cores could be simply regulated by controlling pH. Moreover, we have demonstrated that the amount of functional molecules released from the micellar cores can also be controlled by temperature around the LCST of coronal chains. Such an increment can be correlated with temperature-induced conformational changes on the coronal chains facilitating the release of preloaded functional molecules.

This study significantly contributes to the fundamental understanding of the chemical structure–property relationship of hydrogen-bonded LbL films and may serve as a model study for pH-controlled release of multiple molecules from a single surface-attached film.

Acknowledgements

Authors thank Prof. Mehmet Ali Gulgun and Dr Cinar Oncel at Sabanci University for cross-sectional SEM imaging. V.B. and A.L.D. acknowledge the financial support of Turkish Academy of Sciences. I.E. acknowledges the financial support of L'Oréal-Turkey For Woman in Science Fellowship and a European Commission Marie Curie International Reintegration Grant.

References

- 1 K. Ariga, J. P. Hill and Q. Ji, *Phys. Chem. Chem. Phys.*, 2007, **9**, 2319.
- 2 Z. Tang, Y. Wang, P. Podsiadlo and N. A. Kotov, *Adv. Mater.*, 2006, **18**, 3203.
- 3 E. Brynda, J. Pachernik, M. Houska, Z. Pientka and P. Dvorak, *Langmuir*, 2005, **21**, 7877.
- 4 J. W. Ostrander, A. A. Mamedov and N. A. Kotov, *J. Am. Chem. Soc.*, 2001, **123**, 1101.
- 5 A. A. Mamedov, A. Belov, M. Giersig, N. N. Mamedova and N. A. Kotov, *J. Am. Chem. Soc.*, 2001, **123**, 7738.
- 6 Z. Tang, Y. Wang, P. Podsiadlo and N. A. Kotov, *Adv. Mater.*, 2006, **18**, 3203.
- 7 W. Stockton and M. Rubner, *Macromolecules*, 1997, **30**, 2717.
- 8 L. Wang, Z. Q. Wang, X. Zhang, J. C. Shen, L. F. Chi and H. Fuchs, *Macromol. Rapid Commun.*, 1997, **18**, 509.
- 9 L. Wang, Y. Fu, Sh. Cui, Zh. Wang, X. Zhang, M. Jiang, L. Chi and H. Fuchs, *Langmuir*, 2000, **16**, 10490.
- 10 S. A. Sukhishvili and S. Granick, *J. Am. Chem. Soc.*, 2000, **122**, 9550.
- 11 S. A. Sukhishvili and S. Granick, *Macromolecules*, 2002, **35**, 301.
- 12 K. Kataoka, A. Harada and Y. Nagasaki, *Adv. Drug Delivery Rev.*, 2001, **47**, 113.
- 13 N. Ma, Y. Wang, Z. Wang and X. Zhang, *Langmuir*, 2006, **22**, 3906.
- 14 N. Ma, Y. Wang, B. Wang, Z. Wang and X. Zhang, *Langmuir*, 2007, **23**, 2874.
- 15 J. Cho, J. Hong, K. Char and F. Caruso, *J. Am. Chem. Soc.*, 2006, **128**, 9935.
- 16 P. M. Nguyen and P. T. Hammond, *Langmuir*, 2006, **22**, 7825.

- 17 P. M. Nguyen, N. S. Zacharia, E. Verploegen and P. T. Hammond, *Chem. Mater.*, 2007, **19**, 5524.
- 18 H. Lee, J. A. Lee, Z. Poon and P. T. Hammond, *Chem. Commun.*, 2008, 3726.
- 19 B.-S. Kim, S. W. Park and P. T. Hammond, *ACS Nano*, 2008, **2**, 386.
- 20 Y. Zhao, J. Bertrand, X. Tong and Y. Zhao, *Langmuir*, 2009, **25**, 13151.
- 21 W. S. Tan, R. E. Cohen, M. F. Rubner and S. A. Sukhishvili, *Macromolecules*, 2010, **43**, 1950.
- 22 Z. Zhu and S. A. Sukhishvili, *ACS Nano*, 2009, **3**, 3595.
- 23 G. B. Webber, E. J. Wanless, S. P. Armes, Y. Tang, Y. Li and S. Biggs, *Adv. Mater.*, 2004, **16**, 1794.
- 24 C. Schatz, E. G. Smith, S. P. Armes and E. J. Wanless, *Langmuir*, 2008, **24**, 8325.
- 25 T. Addison, O. J. Cayre, S. Biggs, S. P. Armes and D. York, *Langmuir*, 2008, **24**, 13328.
- 26 S. Biggs, K. Sakai, T. Addison, A. Schmid, S. P. Armes, M. Vamvakaki, V. Bütün and G. B. Webber, *Adv. Mater.*, 2007, **19**, 247.
- 27 E. G. Smith, G. B. Webber, K. Sakai, S. Biggs, S. P. Armes and E. J. Wanless, *J. Phys. Chem. B*, 2007, **111**, 5536.
- 28 K. Sakai, G. B. Webber, C.-D. Vo, E. J. Wanless, M. Vamvakaki, V. Bütün, S. P. Armes and S. Biggs, *Langmuir*, 2008, **24**, 116.
- 29 I. Erel, Z. Zhu, A. Zhuk and S. A. Sukhishvili, *J. Colloid Interface Sci.*, 2011, **355**, 61.
- 30 I. Erel-Unal and S. A. Sukhishvili, *Macromolecules*, 2008, **41**, 3962.
- 31 B.-S. Kim, H. -il Lee, Y. Min, Z. Poon and P. T. Hammond, *Chem. Commun.*, 2009, 4194.
- 32 V. Bütün, S. Sonmez, S. Yarligan, F. F. Taktak, A. Atay and S. Bütün, *Polymer*, 2008, **49**, 4057.
- 33 V. Bütün, S. P. Armes and N. C. Billingham, *Polymer*, 2001, **42**, 5993.
- 34 V. Bütün, N. C. Billingham and S. P. Armes, *J. Am. Chem. Soc.*, 1998, **120**, 11818.
- 35 C. Laurence and M. Berthelot, *Perspect. Drug Discovery Des.*, 2000, **18**, 39.
- 36 Ph. Lavalle, C. Gergely, F. J. G. Cuisinier, G. Decher, P. Schaaf, J. C. Voegel and C. Picart, *Macromolecules*, 2002, **35**, 4458.
- 37 B. Schoeler, E. Poptoshev and F. Caruso, *Macromolecules*, 2003, **36**, 5258.
- 38 J. Ruths, F. Essler, G. Decher and H. Riegler, *Langmuir*, 2000, **16**, 8871.
- 39 P. Bieker and M. Schonhoff, *Macromolecules*, 2010, **43**, 5052.
- 40 L. Kolarik, D. N. Furlong, H. Joy, C. Struijk and R. Rowe, *Langmuir*, 1999, **15**, 8265.
- 41 C. Picart, J. Mutterer, L. Richert, Y. Luo, G. D. Prestwich, P. Schaaf, J.-C. Voegel and P. Lavalle, *Proc. Natl. Acad. Sci. U. S. A.*, 2002, **99**, 12531.
- 42 S. S. Shiratori and M. F. Rubner, *Macromolecules*, 2000, **33**, 4213.
- 43 E. Kharlampieva and S. A. Sukhishvili, *J. Macromol. Sci., Part C*, 2006, **46**, 1.
- 44 IUPAC. Compendium of Chemical Terminology, 2nd ed. (*the "Gold Book"*). Compiled by A. D. McNaught and A. Wilkinson. Blackwell Scientific Publications, Oxford (1997).
- 45 S. Searles and M. Tamres, *J. Am. Chem. Soc.*, 1951, **73**, 3704.
- 46 E. Kharlampieva and S. A. Sukhishvili, *Langmuir*, 2003, **19**, 1235.
- 47 T. Mauser, C. Dejngnat, H. Mohwald and G. B. Sukhorukov, *Langmuir*, 2006, **22**, 5888.
- 48 Z. Sui and J. B. Schlenoff, *Langmuir*, 2004, **20**, 6026.
- 49 I. Erel-Unal and S. A. Sukhishvili, *Macromolecules*, 2008, **41**, 8737.